Knockdown of long non-coding RNA HCP5 suppresses the malignant behavior of retinoblastoma by sponging miR-3619-5p to target HDAC9

YUGUANG ZHU and FENGQIN HAO

Department of Ophthalmology, Affiliated Hospital of Weifang Medical University, Weifang, Shandong 261041, P.R. China

Received September 18, 2020; Accepted January 19, 2021

DOI: 10.3892/ijmm.2021.4907

Abstract. A number of studies have verified the vital effects of long non-coding RNAs on the malignant behaviour of retinoblastoma (RB). The objective of the present study was to examine the specific role and mechanisms of HLA complex P5 (HCP5) in RB. For this purpose, reverse transcription-quantitative polymerase chain reaction was used to determine the expression of HCP5, microRNA (miRNA/miR)-3619-5p and histone deacetylase 9 (HDAC9). A 3-(4,5-dimethyl-2-thiazolyl)-2,5-diphenyl-2-H-tetrazolium bromide assay was conducted to detect cell viability. Transwell assays were used to evaluate the abilities of cell migration and invasion. A mouse tumor model was established to explore the functions of HCP5 in RB *in vivo*. The interactions between HCP5, miR-3619-5p and HDAC9 were confirmed by a dual-luciferase reporter assay. The protein expression of HDAC9 was determined by western blot analysis. The results revealed that the expression levels of HCP5 and HDAC9 were upregulated, whereas those of miR-3619-5p were downregulated in RB tissues and cell lines. The downregulation of HCP5 or the overexpression of miR-3619-5p suppressed RB cell proliferation, migration and invasion *in vitro*. Simultaneously, the knockdown of HCP5 suppressed tumor growth in mice *in vivo*. In addition, HCP5 was directly bound to miR-3619-5p and inversely correlated with miR-3619-5p. *HDAC9* was found to be a target gene of and negatively regulated by miR-3619-5p. HCP5 expression also positively correlated with HDAC9 expression. Rescue experiments revealed that the overexpression of HDAC9 or the inhibition of miR-3619-5p reversed the inhibition of RB cell viability, migration and invasion induced by the knockdown of HCP5. On the whole, the present study demonstrates that the silencing of HCP5 exerts an anti-tumor effect in RB by sponging miR-3619-5p to target HDAC9.

Correspondence to: Dr Fengqin Hao, Department of Ophthalmology, Affiliated Hospital of Weifang Medical University, 2428 Yuhe Road, Weifang, Shandong 261041, P.R. China
E-mail: hao889051@163.com

Abbreviations: lncRNAs, long non-coding RNAs; RB, retinoblastoma; RT-qPCR, reverse transcription-quantitative polymerase chain reaction; DLR, dual-luciferase reporter

Key words: retinoblastoma, long non-coding RNA, HLA complex P5, miR-3619-5p, histone deacetylase 9

Introduction

Retinoblastoma (RB) is an eye malignancy that affects children primarily triggered by mutations in RB genes, the aberrant expression of intracellular molecules and by the activation of oncogenic pathways during the development of the retina (1-3). Approximately 8,000 children are diagnosed with RB each year (4). The clinical symptoms of RB include white pupillary reflex, conjunctival congestion, vitreous opacity, corneal edema, strabismus and increasing intraocular pressure (5,6). Currently, focal therapy (laser and cryotherapy), surgery and chemotherapy are the major treatment strategies for RB (7,8). RB can be cured over time with a graduated-intensity approach based on pathology in developed or even developing countries (9-11). However, the therapeutic effect remains unsatisfactory for children with metastatic and/or advanced RB (9). Therefore, the development of novel targets at the molecular level for RB therapy is crucial.

Long non-coding RNAs (lncRNAs), a type of non-coding RNA composed of >200 nucleotides, regulate the expression of genes by regulating transcription, post-transcription and chromatin modifications (12,13). lncRNAs function as important regulators in the progression of RB (14-16). For instance, the overexpression of lncRNA RB-associated transcript-1 can accelerate the tumorigenesis of RB (14). The downregulation of lncRNA ILF3 antisense RNA 1 and lncRNA LINC00324 has been shown to suppress the proliferation and invasion of RB cells, as well as tumor growth in mice (15,16). lncRNA HLA complex P5 (HCP5), a member of the new pseudogene family P5 (17), is mainly expressed in the immune system, such as in the spleen, blood and thymus (18). HCP5 plays a role in the progression of several types of human cancers (19-21). The study by Bai *et al* indicated that the downregulation of HCP5 suppressed the viability, migration and invasion of colorectal cancer (CRC) cells and impeded the malignant behavior of CRC *in vivo* (19). Wang *et al* revealed that the knockdown of HCP5 exerted an inhibitory effect on the growth and metastasis of ovarian cancer (OC) in mice (20). Similarly, Yuan *et al* suggested that the progression of pancreatic cancer

was significantly suppressed by the silencing of HCP5 (21). Nevertheless, the specific role and potential mechanisms of HCP5 in RB are relatively unknown.

The participation of microRNAs (miRNAs or miRs) in the pathogenesis of RB has been uncovered (22,23). Wan *et al* reported that miR-25-3p exertd a protective effect against RB tumorigenesis by dampening the proliferation, migration and invasion of RB (22). Li and You demonstrated that miR-758 functioned as a suppressor of the metastasis of RB (23). Recent studies demonstrated that miR-3619-5p played an anti-tumor role in liver cancer and RB (24,25). More importantly, the interaction of miR-3619-5p with lncRNA LINC00202 has been shown to considerably contribute to the suppression of the progression of RB (25). It remains unclear however, as to whether the inhibitory effect of miR-3619-5p in RB tumorigenesis is modulated by HCP5.

Histone deacetylase 9 (HDAC9), a member of class II HDACs, possesses a conserved domain of HDAC and can interact with tissue-specific transcription factors and co-repressors (26). In recent years, the carcinogenesis of HDAC9 in RB has attracted increasing attention (27-29). Both Zhang *et al* (27) and Xu *et al* (29) suggested that the down-regulation of HDAC9 suppressed the proliferation of RB cells, thus, attenuating RB *in vitro* (27,29). Jin *et al* revealed that the overexpression of HDAC9 reversed the anti-proliferative effect of miR-101-3p on RB cells (28). Nevertheless, the interactions between miR-3619-5p and HDAC9, as well as the HCP5/miR-3619-5p/HDAC9 axis in the progression of RB remain relatively unknown.

The present study thus focused on investigating the expression and roles of HCP5 and miR-3619-5p in RB, and on exploring the association between HCP5, miR-3619-5p and HDAC9 in RB cells. Collectively, the findings of the present study may provide a novel target for the treatment of RB.

Materials and methods

Collection of samples. RB tissues and adjacent normal tissues in pairs (n=71) were obtained from patients who were diagnosed with RB (unilateral, 51; bilateral, 20) from June, 2017 to July, 2019 at the Affiliated Hospital of Weifang Medical University. Among the patients, 41 lymph node metastases and 2 distant metastasis cases (1 cerebral spinal fluid and 1 brain) were included. The tumor node metastasis (TNM) stage (30), intraocular international RB classification (IIRC) stage (31) and Reese Ellsworth (RE) stage (32) were used to classify RB. The present study was conducted in accordance with the Declaration of Helsinki and approved by the Ethics Committee of the Affiliated Hospital of Weifang Medical University [no. 2020(12)]. Written informed consent was obtained from all patients, and parental consent was obtained in cases where the patient was <18 years old.

Cells and cell culture. A human normal retinal pigmented epithelium cell line (APRE-19) and 4 human RB cell lines (Y79, HXO-RB44, WERI-Rb-1 and SO-RB50) were purchased from the American Type Culture Collection (ATCC). The ARPE-19 cells were cultured in Dulbecco's modified Eagle's medium (Invitrogen; Thermo Fisher Scientific, Inc.) containing 10% fetal bovine serum (FBS; Gibco; Thermo Fisher Scientific, Inc.). The Y79, Weri-RB1, SO-RB50 and HXO-RB44 cells were cultured in modified Roswell Park Memorial Institute-1640 medium (Gibco; Thermo Fisher Scientific, Inc.) containing 10% FBS. All cells were incubated at 37˚C in a humidified atmosphere with 5% CO_2.

Reverse transcription-quantitative polymerase chain reaction (RT-qPCR). Total RNA isolated from the tissues or cells was analyzed using TRIzol reagent (Invitrogen; Thermo Fisher Scientific, Inc.). The extracted RNA was reverse transcribed into complementary DNA (cDNA) using a Prime-Script RT reagent kit (Takara Biotechnology Co., Ltd.). Subsequently, SYBR® Premix Ex Taq™ II (Takara Biotechnology Co., Ltd.) was utilized for the amplification of cDNA. The reaction conditions were 95˚C for 5 min, 40 cycles of 95˚C for 15 sec, 60˚C for 20 sec, and 70˚C for 15 sec. The primer sequences used in the present study are listed in Table I. The relative expression of HCP5, miR-3619-5p and HDAC9 was calculated using the $2^{-\Delta\Delta Cq}$ method (33). The endogenous controls were U6 and GAPDH.

Cell transfection. Short hairpin (sh) RNA against HCP5 (sh-HCP5), sh-negative control (sh-NC), miR-NC and miR-3619-5p mimics, as well as miR-3619-5p inhibitor, pcDNA-HDAC9, pcDNA-MS2, pBobi-MS2-GFP and pcDNA-HCP5-MS2 were purchased from Guangzhou RiboBio Co., Ltd. sh-HCP5 or sh-NC were firstly cloned into a lentiviral vector. These factors (all, 50 nM) were then transfected into Y79 and/or HXO-RB44 cells using Lipofectamine 3000 (Invitrogen; Thermo Fisher Scientific, Inc.). Then, 48 h after transfection, the cells were harvested for further experiments.

Target prediction. The target miRNAs of HCP5 were predicted using StarBase v2.0 software (http://starbase.sysu.edu.cn). A total of 8 miRNAs (miR-3681-3p, miR-29b-3p, miR-520a-5p, miR-3619-5p, miR-216a-3p, miR-20b-5p, miR-128-3p, and miR-4701-5p) were selected for verification via RNA immunoprecipitation (RIP) assay. Similarly, the target genes of miR-3619-5p were also predicted using StarBase v2.0 software. HDAC9 was selected due to its important role in RB.

RIP assay. pcDNA-MS2, pBobi-MS2-GFP and pcDNA-HCP5-MS2 were transfected into the Y79 or HXO-RB44 cells. The RIP assay was performed with anti-GFP antibody (1:5,000; ab6673, Abcam), as well as a MagnaRIP RNA-Binding Protein Immunoprecipitation kit (EMD Millipore). The expression of the aforementioned miRNAs was detected by RT-qPCR.

Dual luciferase reporter (DLR) assay. The 3'-UTR fragment of HCP5, including the predicted or mutated binding site for miR-3619-5p, was introduced into psiCHECK2 (Promega Corporation) to establish HCP5 wild-type (wt) or HCP5 mutant-type (mut). Similarly, the 3'-UTR sequence of HDAC9 containing the predicted or mutated binding site for miR-3619-5p was inserted into psiCHECK2 (Promega Corporation) to construct HDAC9 wt or mut. For reporter assays, one of the above-mentioned vectors (80 ng) along with miR-3619-5p mimics or miR-NC (50 nM) were co-transfected into the Y79 and HXO-RB44 cells using Lipofectamine 3000

Table I. Primer sequences used for RT-qPCR in the present study.

Gene	Forward	Reverse
HCP5	5'-CCGCTGGTCTCTGGACACATACT-3'	5'-CTCACCTGTCGTGGGATTTTGC-3'
miR-3619-5p	5'-UCAGCAGGCAGGCUGGUGCAGC-3'	5'-GCUGCACCAGCCUGCCUGCUGA-3'
HDAC9	5'-ATGGTTTCACAGCAACGCATT-3'	5'-ACCTTGCCTAAGCGTCTGC-3'
GAPDH	5'-GGAGCGAGATCCCTCCAAAAT-3'	5'-GGCTGTTGTCATACTTCTCATGG-3'
U6	5'-TCCGATCGTGAAGCGTTC-3'	5'-GTGCAGGGTCCGAGGT-3'

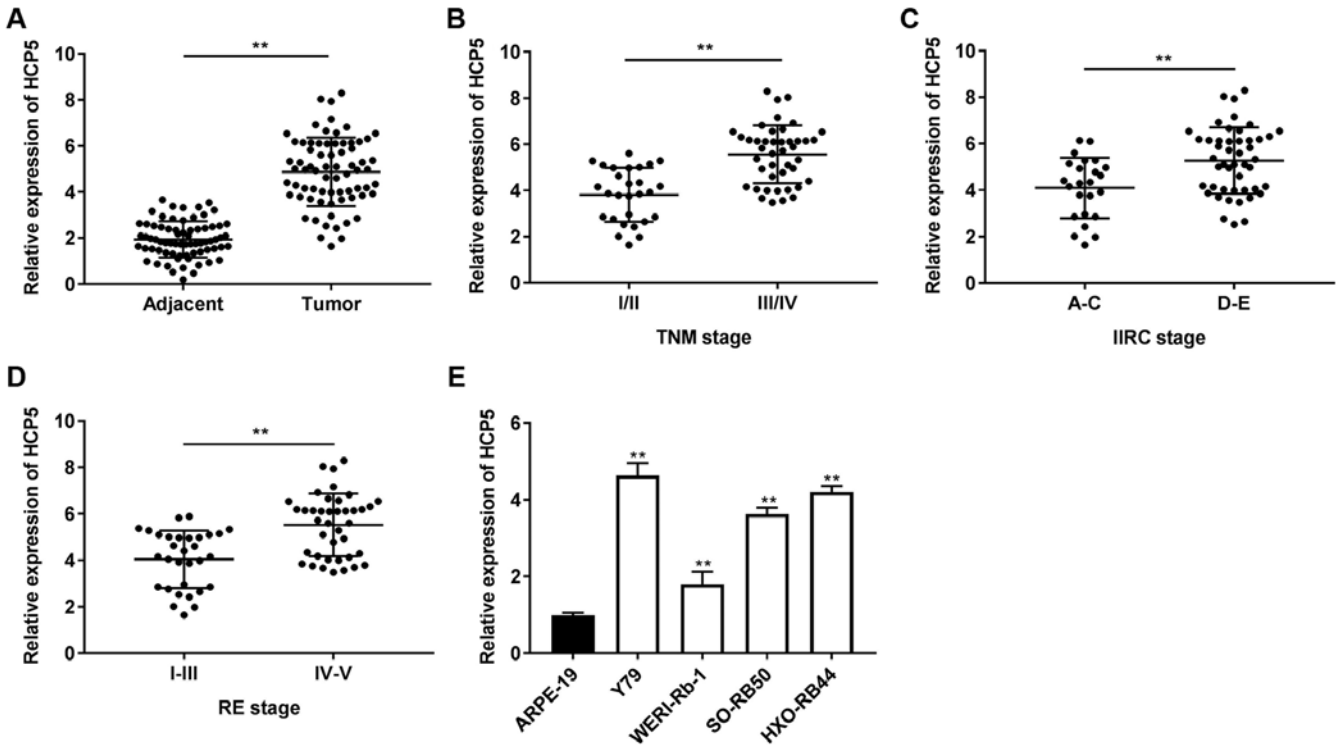

Figure 1. lncRNA HCP5 is highly expressed in retinoblastoma tissues and cells. (A) Relative expression of HCP5 in tumor tissues and adjacent normal tissues was determined by RT-qPCR. **P<0.01, vs. adjacent normal tissues. (B) Relative expression of HCP5 in tumors at TNM stage I/II and III/IV was determined by RT-qPCR. **P<0.01, vs. TNM stage I/II. (C) Relative expression of HCP5 in IIRC stage A/B/C and IIRC stage D/E was determined by RT-qPCR. **P<0.01, vs. IIRC stage A/B/C. (D) Relative expression of HCP5 in RE stage I/II/III and RE stage IV/V was determined by RT-qPCR. **P<0.01, vs. RE stage I/II/III. (E) Relative expression of HCP5 in ARPE-19, Y79, HXO-RB44, WERI-Rb-1 and SO-RB50 cells was determined by RT-qPCR. **P<0.01, vs. ARPE-19 cells. The experiments were performed in triplicate and repeated 3 times. Data are presented as the means ± standard deviation (SD). TNM, tumor node metastasis; IIRC, intraocular international retinoblastoma classification; RE, Reese Ellsworth.

(Invitrogen; Thermo Fisher Scientific, Inc.). Following transfection for 48 h, relative luciferase activity was examined using a DLR assay System (Promega Corporation). The activity of Firefly luciferase was normalized to that of *Renilla* luciferase.

3-(4,5-Dimethyl-2-thiazolyl)-2,5-diphenyl-2-H-tetrazolium bromide (MTT) assay. The transfected cells were plated into 96-well plates at a density of 5,000 cells/well and cultured for 48 h at 37˚C. MTT reagent (20 μl; Sigma-Aldrich; Merck KGaA) was then added to each well at different time points (24, 48, 72 and 96 h) followed by incubation for 4 h at 37˚C. After discarding the medium, 150 μl of dimethyl sulfoxide (Sigma-Aldrich; Merck KGaA) were added to each well. The optical density was measured at 490 nM using an enzyme immunoassay instrument (Bio-Tek Instruments, Inc.).

Cell migration and invasion assays. The 24-well Transwell chambers (8 μM pore size; BD Biosciences) coated with Matrigel (BD Biosciences) were used to evaluate cell invasion. Cells ($1x10^5$) were resuspended in 200 μl of serum-free medium and then plated into the upper chambers of each Transwell apparatus. A total of 600 μl of medium containing 10% FBS was added to the lower chambers followed by incubation at 37˚C for 48 h. Subsequently, the cells in the upper chambers were wiped off using a cotton swab, and those adhering to the lower chambers were fixed with 4% paraformaldehyde and stained with 0.5% crystal violet (TCI chemicals) at 37˚C for 30 min. Stained cells were imaged using an inverted light microscope (Olympus Corporation) and analyzed using ImageJ software [version 1.46, National Institutes of Health (NIH)].

Table II. Clinical parameters of the patients with retinoblastoma included in the present study.

Variable	Total	HCP5 expression		P-value
		Low (n=35)	High (n=36)	
Age				0.540
<3 years	40	21	19	
≥3 years	31	14	17	
Sex				0.124
Male	32	19	13	
Female	39	16	23	
Tumor size (mm)				0.546
<10	38	20	18	
≥10	33	15	18	
TNM stage				0.003[b]
I/II	28	20	8	
III/IV	43	15	28	
Lymph node metastasis				0.043[a]
No	30	19	11	
Yes	41	16	25	
Distant metastasis				
No	69	35	34	0.157
Yes	2	0	2	
Laterality				0.131
Unilateral	51	28	23	
Bilateral	20	7	13	
IIRC stage				0.009[b]
A/B/C	24	17	7	
D/E	47	18	29	
RE stage				0.024[a]
I/II/III	31	20	11	
IV/V	40	15	25	

[a]P<0.05, [b]P<0.01. TNM, tumor node metastasis; IIRC, Intraocular International Retinoblastoma classification; RE, Reese Ellsworth.

For the cell migration assay, the procedure was similar to the cell invasion assay, except that the 24-well Transwell chambers were not pre-coated with Matrigel.

Western blot analysis. Total protein was extracted from the transfected Y9 and/or HXO-RB44 cells using RIPA lysis buffer (Beyotime Institute of Biotechnology). The protein concentration was detected using the BCA Protein Assay kit (Abcam). Proteins were separated by 10% sodium dodecyl sulphate-polyacrylamide gel electrophoresis and transferred onto polyvinylidene fluoride membranes (MilliporeSigma). The membranes were then blocked with 5% non-fat milk for 2 h followed by incubation with the primary antibodies anti-HDAC9 (1:1,000; ab109446, Abcam) and anti-GAPDH (1:1,000; ab9485, Abcam) overnight at 4˚C. Tris-buffered saline Tween-20 was then used to wash the membranes 3 times. Subsequently, HRP-conjugated anti-rabbit IgG secondary antibody (1:5,000; ab205718, Abcam) was added followed by incubation for 1 h at 37˚C. Finally, protein bands were visualized using an enhanced chemiluminescence system (Thermo Fisher Scientific, Inc.). The relative protein expression over GAPDH was quantified using Alpha Innotech imaging software (ProteinSimple).

Xenograft tumor model. Female BALB/c nude mice (4-5 weeks of age, weighing 20-25 g) were obtained from the Shanghai Laboratory Animal Centre (Shanghai, China). All mice were housed under controlled conditions (25˚C, 50% humidity, 12 h light/dark cycle) and were provided with free access to food and water. Subsequently, the mice were randomly divided into the 2 following groups: The sh-NC group (n=5) and the sh-HCP5 group (n=5). sh-HCP5 or sh-NC were integrated into a lentiviral vector and transfected into the Y79 cells. Furthermore, the transfected Y79 cells ($2x10^6$ cells/100 μl, s.c.) were injected into the right flanks of the nude mice. Tumor volumes were measured every other week using the following formula: $(A \times B^2)/2$, (A, the longest diameter; B, the shortest diameter). After 4 weeks, the mice

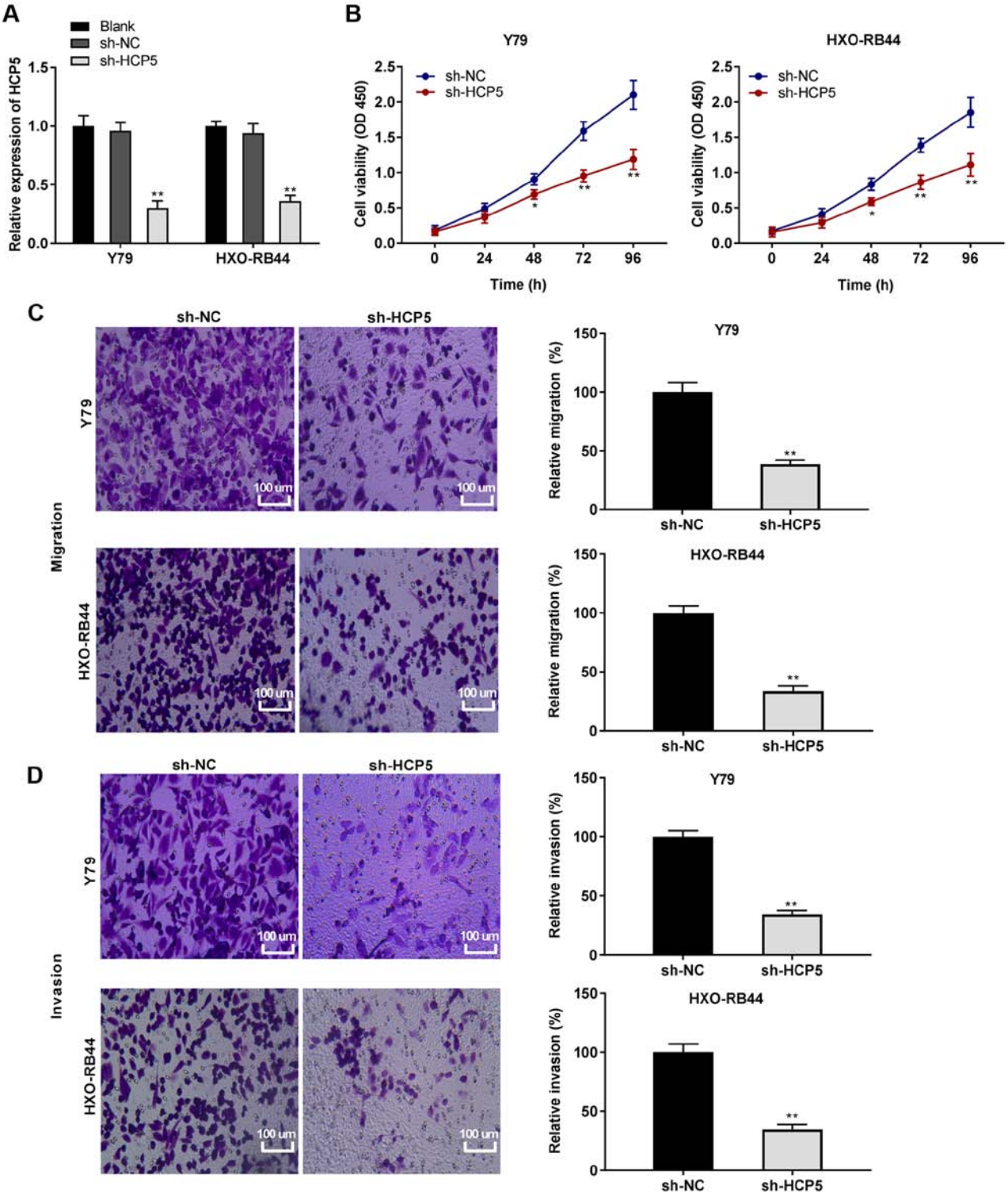

Figure 2. Silencing of lncRNA HCP5 suppresses the viability, migration and invasion of retinoblastoma cells. (A) Following transfection with short hairpin (sh)-HCP5 and sh-negative control (sh-NC), the relative expression of HCP5 in Y79 and HXO-RB44 cells was detected by RT-qPCR. **P<0.01, vs. sh-NC. (B) Following transfection with sh-HCP5 and sh-NC, the viability of Y79 and HXO-RB44 cells was detected MTT assay. *P<0.05, **P<0.01, vs. sh-NC. (C) Following transfection with sh-HCP5 and sh-NC, the relative migration of Y79 and HXO-RB44 cells was detected by Transwell assay; magnification, x400; scale bar, 100 μm; **P<0.01, vs. sh-NC. (D) Following transfection with sh-HCP5 and sh-NC, the relative invasion of Y79 and HXO-RB44 cells was detected by Transwell assay; magnification, x400; scale bar, 100 μm; **P<0.01, vs. sh-NC. The *in vitro* experiments were performed in triplicate and repeated 3 times. Data are presented as the means ± standard deviation (SD). HCP5, HLA complex P5.

were anaesthetized with pentobarbital sodium (50 mg/kg) and euthanized by cervical dislocation. The tumor xenografts were separated from the mice and weighed. The animal experiments were approved by the Ethics Committee of the Affiliated Hospital of Weifang Medical University [no. 2020(12)] and were performed in accordance with the institutional guide for the care and use of laboratory animals (National Institutes of Health).

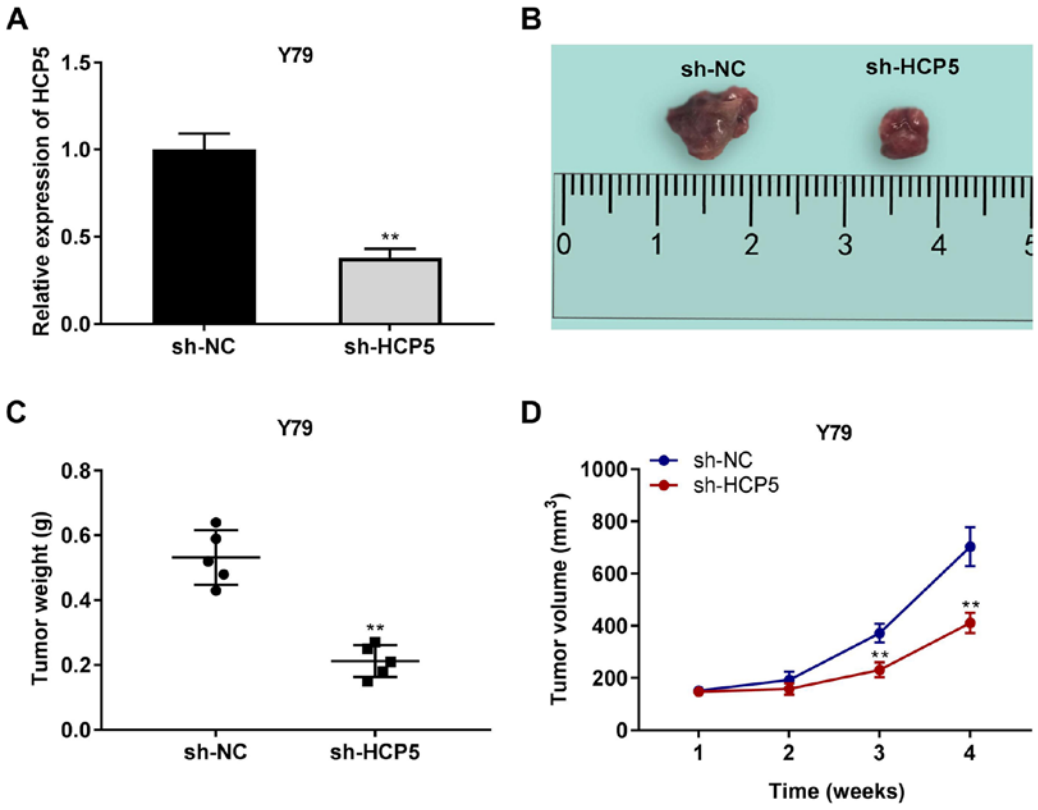

Figure 3. Silencing of lncRNA HCP5 suppresses the growth of tumor xenografts *in vivo*. (A) The expression of HCP5 in mouse tissues was detected by RT-qPCR. **P<0.01, vs. sh-NC. (B) Image of solid tumors after the injection of sh-HCP5 or sh-NC. (C) Weight of tumor xenografts after the injection of sh-HCP5 or sh-NC. **P<0.01, vs. sh-NC. (D) Volume of tumor xenografts after the injection of sh-HCP5 or sh-NC. **P<0.01, vs. sh-NC. The *in vivo* experiments were performed in 5 mice in each group. Data are presented as the means ± standard deviation (SD). HCP5, HLA complex P5.

Statistical analysis. *In vitro* experiments were performed in triplicate, and each experiment was repeated 3 times. *In vivo* experiments were performed using 5 mice per group. Statistical analyses were performed using SPSS Statistics 22.0. The Student's t-test was used for comparisons between 2 groups (paired t-test for the data in Figs. 1A, 4E, and 6C; unpaired t-test for the data in Figs. 1B, C, D, 2C, D, 3A, C, 4D, 5C, D and 6F). One-way ANOVA was used to assess differences among multiple groups, followed by Tukey's post hoc test. Pearson's correlation analysis was used to determine the correlation between HCP5 and miR-3619-5p expression, as well as that between miR-3619-5p and HDAC9, and HDAC9 and HCP5 expression in RB tissues. Data are presented as the means ± standard deviation (SD). The Chi-squared test was used to analyze the categorical data presented in Table II. Statistically significant differences were regarded as those with values of P<0.05.

Results

lncRNA HCP5 is highly expressed in RB tissues and cells. First, the expression of HCP5 was determined by RT-qPCR and it was found that the expression of HCP5 in the tumor tissues was distinctly increased compared to that in adjacent tissues (P<0.01; Fig. 1A). Subsequently, the association between HCP5 expression and the pathological features of RB cases was analyzed. It was found that a high and low expression of HCP5 exhibited significant differences in TNM stage (P=0.003), lymph node metastasis (P=0.043), IIRC stage (P=0.009) and RE stage (P=0.024) (Table II). As illustrated in Fig. 1B-D, an increased expression of HCP5 was observed in TNM stage III/IV, IIRC stage D/E and RE stage IV/V (P<0.01), compared to TNM stage I/II, IIRC stage A/C and RE stage I/II/III, respectively. The expression of HCP5 was also determined in RB cells and an elevated expression of HCP5 was found in the Rb cell lines (Y79, HXO-RB44, WERI-Rb-1 and SO-RB50) (P<0.01; Fig. 1E). In addition, a relatively higher expression of HCP5 was found in the HOX-RB44 and Y79 cell lines among the 4 RB cell lines. Therefore, the HOX-RB44 and Y79 cells were used in the following experiments.

Silencing of lncRNA HCP5 suppresses the viability, migration and invasion of RB cells. To explore the function of HCP5 in RB cells, the transfection efficiency of sh-HCP5 in both the HXO-RB44 and Y79 cell lines was initially detected. Transfection with sh-HCP5 markedly reduced the expression of HCP5 (all P<0.01; Fig. 2A). Subsequently, functional experiments were conducted on HCP5. MTT assay revealed that transfection with sh-HCP5 led to a notable decrease in the viability of the HXO-RB44 and Y79 cells (P<0.05; Fig. 2B). Additionally, the relative migration and invasion of the Y79 and HXO-RB44 cells were reduced by the knockdown of HCP5 (all P<0.01; Fig. 2C and D).

Silencing of lncRNA HCP5 suppresses the growth of tumor xenografts in vivo. The expression of HCP5 in mouse tissues

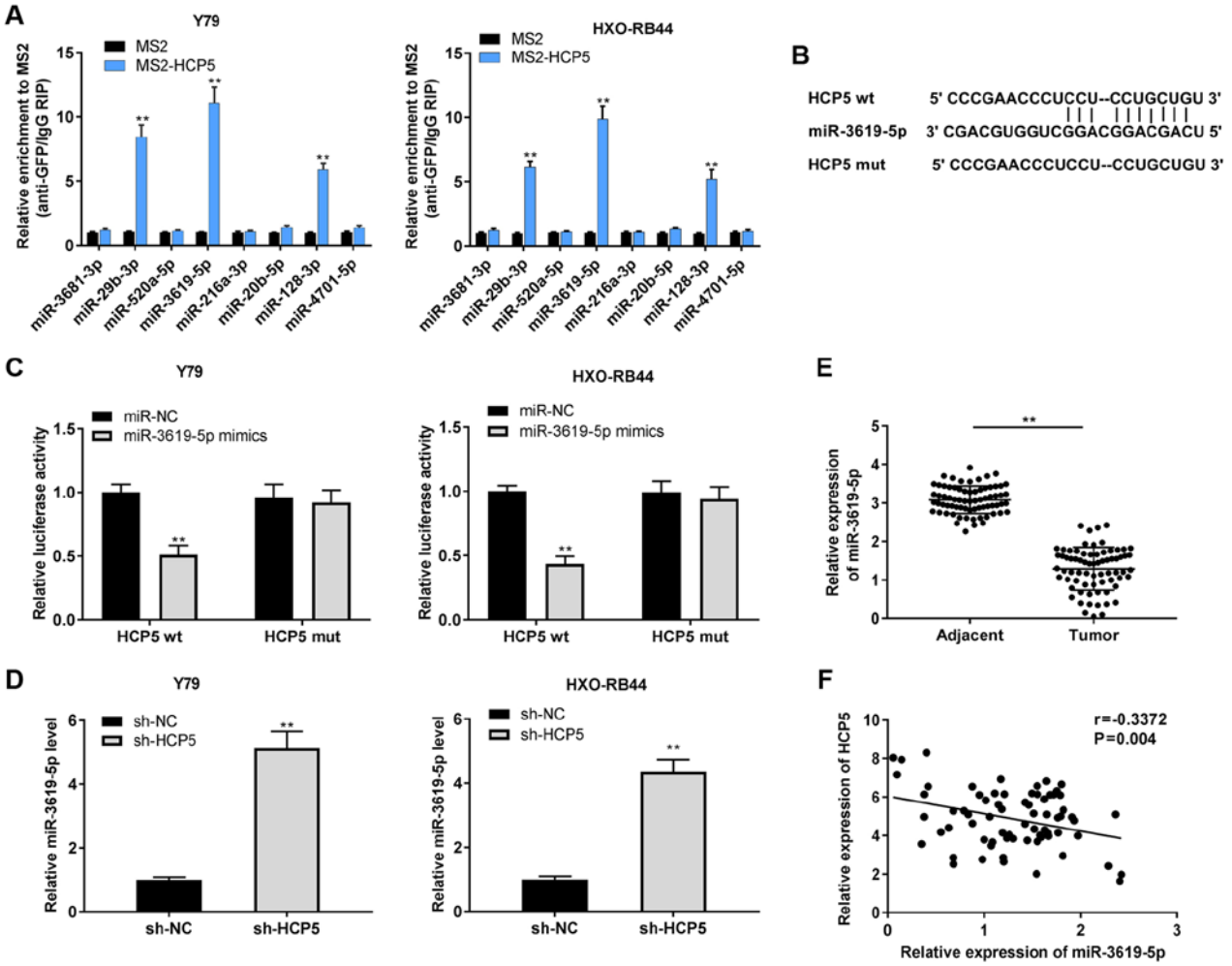

Figure 4. HCP5 serves as a competing endogenous RNA for miR-3619-5p. (A) RIP assay was used for assessing miRNAs associated with HCP5. **P<0.01, vs. MS2. (B) The binding sequence between HCP5 and miR-3619-5p was predicted using StarBase (http://starbase.sysu.edu.cn/). (C) The interaction between HCP5 and miR-3619-5p in Y79 and HXO-RB44 cells was validated by DLR assay. **P<0.01, vs. miR-negative control (NC). (D) Following transfection with sh-HCP5 and sh-NC, the relative expression of miR-3619-5p was detected by RT-qPCR in Y79 and HXO-RB44 cells. **P<0.01, vs. sh-NC. (E) Relative expression of miR-3619-5p in tumor tissues and adjacent normal tissues was detected by RT-qPCR. **P<0.01, vs. adjacent normal tissues. (F) The correlation between HCP5 and miR-3619-5p in retinoblastoma tissues was analyzed by Pearson's correlation analysis. P=0.004; r=-0.3372. The experiments were performed in triplicate and repeated 3 times. Data are presented as the means ± standard deviation (SD). HCP5, HLA complex P5; DLR, dual luciferase reporter.

was also determined. The results of RT-qPCR demonstrated that HCP5 expression was decreased by the injection of sh-HCP5 (P<0.01, Fig. 3A). The effect of sh-HCP5 on tumor xenografts was then examined. As illustrated in Fig. 3B-D, it was found that tumor weight in the sh-HCP5 group was lower than that in the sh-NC group, and the tumor volume was markedly decreased by sh-HCP5 on the 28th day after the injection in mice (P<0.01).

HCP5 serves as a competing endogenous RNA for miR-3619-5p. To explore the regulatory mechanisms of HCP5 in RB, the target miRNAs of HCP5 were predicated using StarBase v2.0 software. RIP assay was performed to verify 8 selected miRNAs. As shown in Fig. 4A, the Y79 and HXO-RB44 cells in the MS2-HCP5 group were enriched with miR-29b-3p, miR-3619-5p and miR-128-3p compared with the MS2 group. Among these 3 miRNAs, miR-3619-5p was selected due to its relatively high enrichment with HCP5. The predicted binding site of HCP5 and miR-3619-5p is shown in Fig. 4B. DLR assay further revealed that the relative luciferase activity of the Y79 and HXO-RB44 cells co-transfected with HCP5 wt and miR-3619-5p mimics was conspicuously lower than that of the Y79 and HXO-RB44 cells co-transfected with HCP5 wt and miR-NC (all P<0.01; Fig. 4C). Subsequently, the effect of HCP5 on miR-3619-5p expression was examined and it was observed that the expression of miR-3619-5p increased following the downregulation of HCP5 in the Y79 and HXO-RB44 cells (all P<0.01; Fig. 4D). Moreover, miR-3619-5p expression in tumor tissues was diminished in comparison with adjacent normal tissues (P<0.01; Fig. 4E). A negative correlation was validated between HCP5 and miR-3619-5p in RB tissues using Pearson's correlation analysis (P=0.004, r=-0.3372; Fig. 4F).

Overexpression of miR-3619-5p inhibits the viability, migration and invasion of RB cells. Accordingly, the role of miR-3619-5p in RB cells was explored; miR-3619-5p mimics and inhibitors were transfected into RB cells. As was expected, miR-3619-5p expression increased by the addition of miR-3619-5p mimics, whereas it was decreased by transfection with miR-3619-5p inhibitor in the HXO-RB44 and Y79 cells (all P<0.01; Fig. 5A). Importantly, it was discovered that the overexpression of

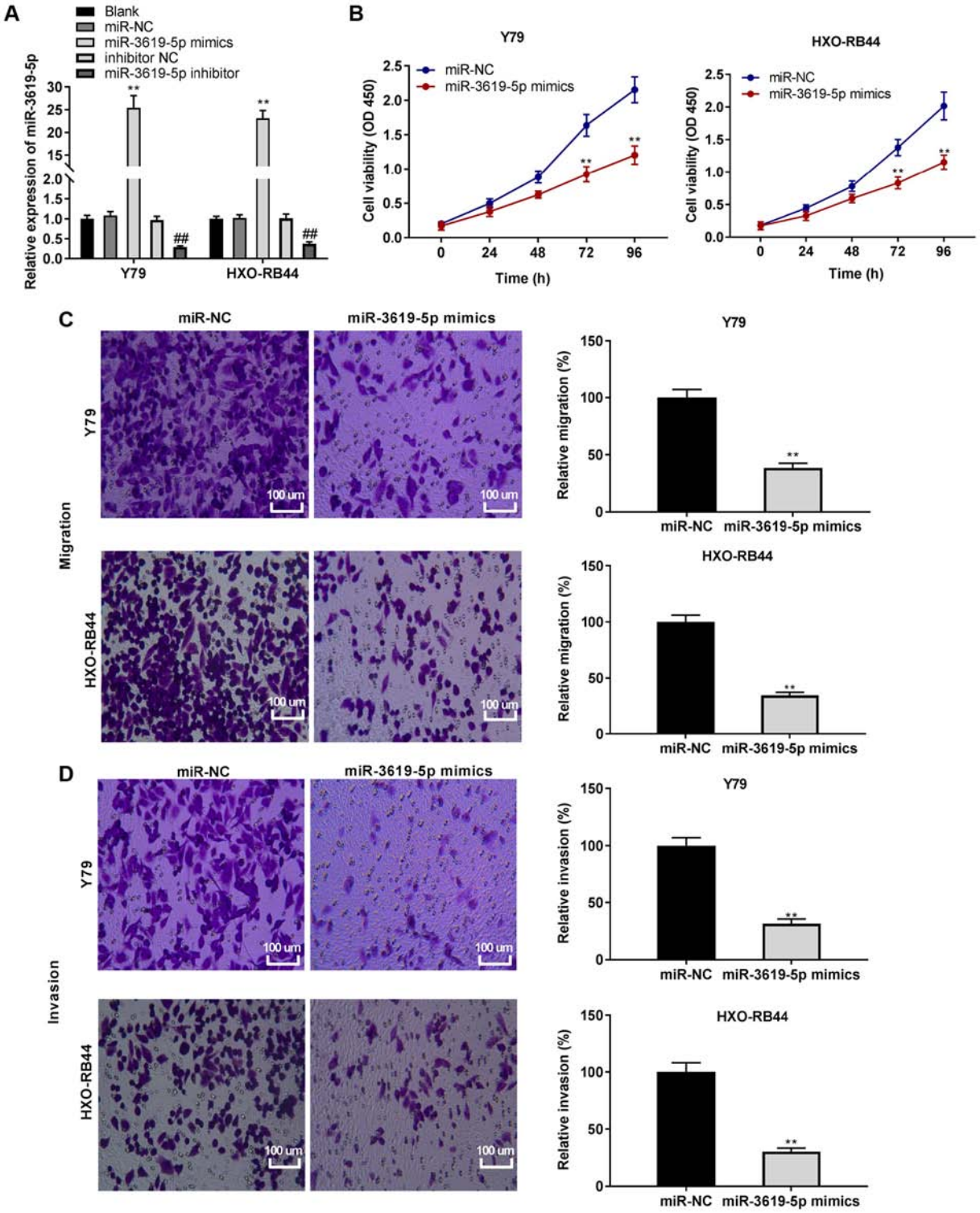

Figure 5. Overexpression of miR-3619-5p inhibits the viability, migration and invasion in retinoblastoma cells. (A) Following transfection with miR-3619-5p mimics/miR-negative control (NC) or miR-3619-5p inhibitor/inhibitor NC, the relative expression of miR-3619-5p was detected by RT-qPCR. **P<0.01, vs. miR-NC. (B) Following transfection with miR-3619-5p mimics and miR-NC, cell viability was determined by MTT assay in Y79 and HXO-RB44 cells. **P<0.01, vs. miR-NC. (C) Following transfection with miR-3619-5p mimics and miR-NC, the relative migration of Y79 and HXO-RB44 cells was determined by Transwell assay; magnification, x400; scale bar, 100 μm; **P<0.01, vs. miR-NC. (D) Following transfection with miR-3619-5p mimics and miR-NC, the relative invasion of Y79 and HXO-RB44 cells was detected by Transwell assay; magnification, x400; scale bar, 100 μm; **P<0.01, vs. miR-NC. The experiments were performed in triplicate and repeated 3 times. Data are presented as the means ± standard deviation (SD).

miR-3619-5p caused a decrease in the viability of the Y79 and HXO-RB44 cells (all P<0.01; Fig. 5B). Moreover, the overexpression of miR-3619-5p suppressed the migration and invasion of the Y79 and HXO-RB44 cells (all P<0.01; Fig. 5C and D).

Identification of HDAC9 as a target gene of miR-3619-5p. To elucidate the mechanisms of miR-3619-5p in the progression of RB, the target gene of miR-3619-5p was predicted using StarBase v2.0 software and it was found that miR-3619-5p

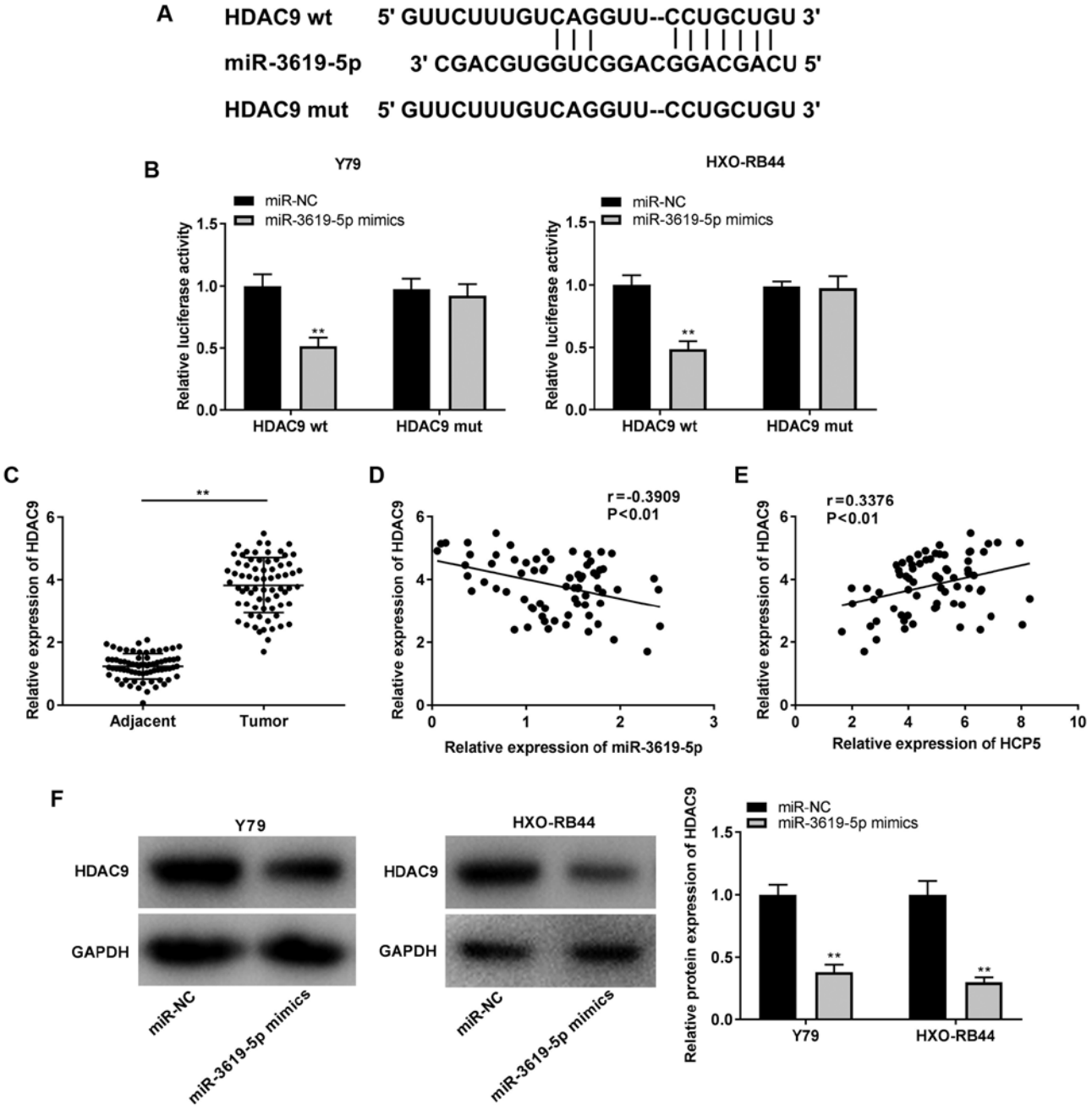

Figure 6. HDAC9 was targeted by miR-3619-5p. (A) The binding sites between HDAC9 and miR-3619-5p were predicted using StarBase (http://starbase.sysu.edu.cn/). (B) DLR assay was used to confirm the targeting association between HDAC9 and miR-3619-5p in Y79 and HXO-RB44 cells. **P<0.01, vs. miR-negative control (NC). (C) Relative expression of HDAC9 in tumor tissues and adjacent normal tissues was detected by RT-qPCR. **P<0.01, vs. adjacent normal tissues. (D) The correlation between HDAC9 and miR-3619-5p in retinoblastoma tissues was analyzed by Pearson's correlation analysis. P<0.01; r=-0.3909. (E) The correlation between HDAC9 and HCP in retinoblastoma tissues was analyzed by Pearson's correlation analysis. P<0.01; r=0.3376. (F) Relative expression of HDAC9 in Y79 and HXO-RB44 cells was detected by RT-qPCR following transfection with miR-3619-5p mimics or miR-NC. **P<0.01, vs. miR-NC. The experiments were performed in triplicate and repeated 3 times. Data are presented as the means ± standard deviation (SD). HCP5, HLA complex P5; HDAC9, histone deacetylase 9; DLR, dual luciferase reporter.

shared a complementary binding sequence at the 3-UTR with HDAC9 (Fig. 6A). Furthermore, the DLR assay verified that transfection with miR-3619-5p mimics markedly reduced the luciferase activity of the HDAC9 wt vector compared with that of miR-NC, whereas it did not exert any significant effect on the luciferase activity of the HDAC9 mut vector in the Y79 and HXO-RB44 cells (all P<0.01; Fig. 6B). Simultaneously, it was discovered that HDAC9 expression was markedly increased in tumor tissues in contrast to adjacent normal tissues (P<0.01; Fig. 6C). Pearson's correlation analysis demonstrated that HDAC9 expression negatively correlated with miR-3619-5p expression (r=-0.3909), and HDAC9 expression positively correlated with HCP5 expression in RB tissues (r=0.3376; all P<0.01; Fig. 6D and E). The regulatory association between miR-3619-5p and HDAC9 was then examined, and it was observed that the relative protein expression of HDAC9 was reduced by the upregulation of miR-3619-5p in the Y79 and HXO-RB44 cells (all P<0.01; Fig. 6F).

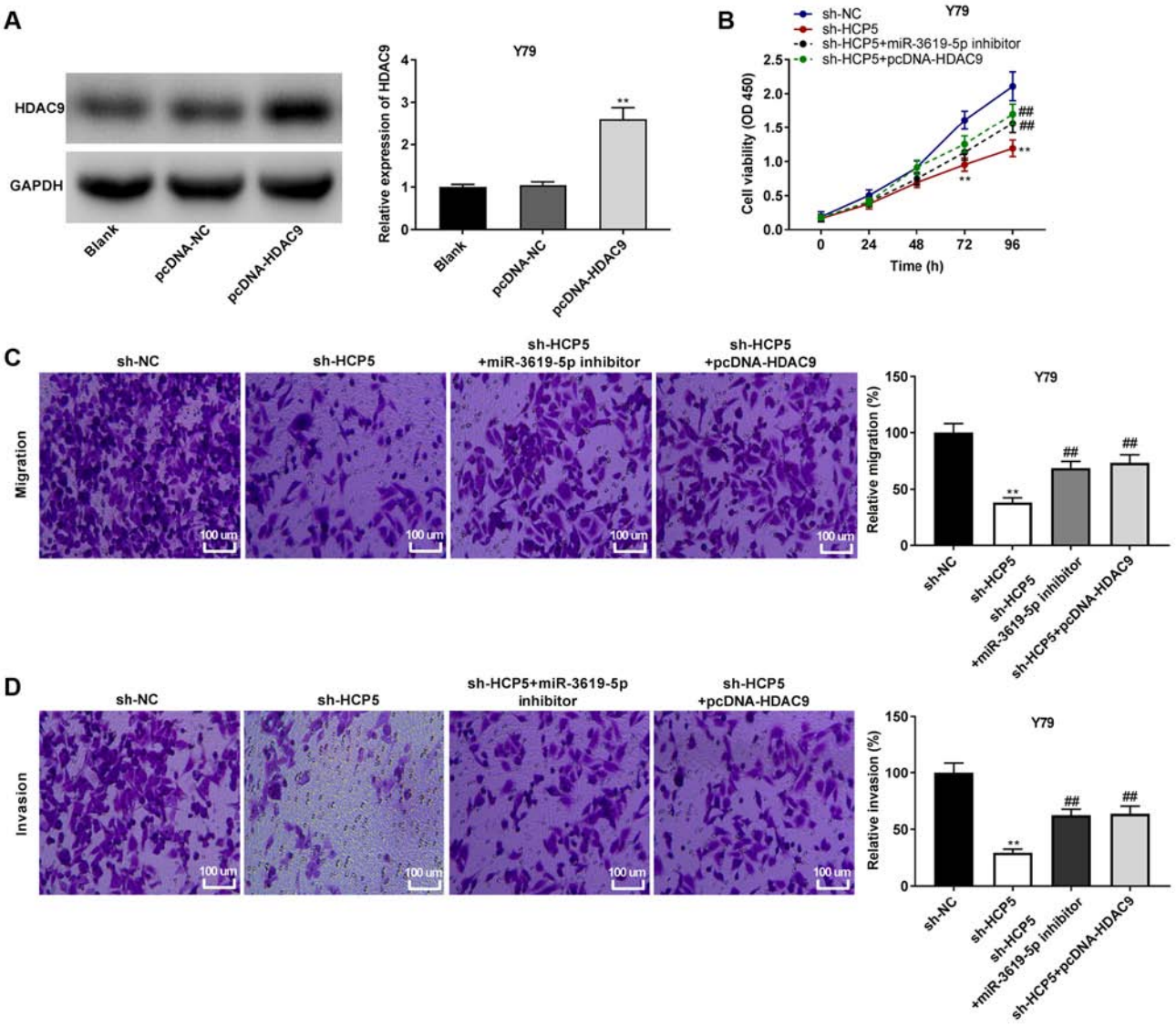

Figure 7. lncRNA HCP5 suppresses cell viability, migration and invasion by sponging miR-3619-5p to target HDAC9. (A) The protein expression of HDAC9 in Y79 cells was detected by western blot analysis. **P<0.01, vs. pcDNA-negative control (NC). (B) Cell viability was determined by MTT assay in Y79 cells. **P<0.01, vs. short hairpin (sh)-NC; ##P<0.01, vs. sh-HCP5. (C) Relative migration of Y79 cells was determined by Transwell assay. Magnification, x400; scale bar, 100 μm; **P<0.01, vs. sh-NC; ##P<0.01, vs. sh-HCP5. (D) Relative invasion of Y79 cells was detected by Transwell assay. Magnification, x400; scale bar, 100 μm; **P<0.01, vs. sh-NC; ##P<0.01, vs. sh-HCP5. The experiments were performed in triplicate and repeated 3 times. Data are presented as the means ± standard deviation (SD). HCP5, HLA complex P5; HDAC9, histone deacetylase 9.

lncRNA HCP5 suppresses RB cell viability, migration and invasion by sponging miR-3619-5p to target HDAC9. Subsequently, Y79 cells with a relatively high expression of HCP5 were used to perform rescue experiments. To investigate whether HCP5 affects RB cells by regulating the miR-3619-5p/HDAC9 axis, HDAC9 was first overexpressed in Y79 cells. As shown in Fig. 7A, HDAC9 expression was markedly upregulated by transfection with pcDNA-HDAC9 in the Y79 cells (P<0.01). Furthermore, rescue assays were performed. MTT assay revealed that cell viability was reduced by transfection with sh-HCP5, while the addition of miR-3619-5p inhibitor or pcDNA-HDAC9 reversed the sh-HCP5-mediated decrease in the viability of Y79 cells (all P<0.01; Fig. 7B). Transwell assays indicated that sh-HCP5 suppressed the migration and invasion of Y79 cells, whereas the suppressive effects of sh-HCP5 on the migratory and invasive abilities were partially eliminated by miR-3619-5p inhibitor or pcDNA-HDAC9 in the Y79 cells (all P<0.01; Fig. 7C and D).

Discussion

RB is an eye malignant tumor that mainly affects children (8). The abnormal expression of lncRNA HCP5 plays a clinically predictive role in tumorigenesis in a number of types of cancer (34-36). For example, HCP5 expression is higher in cervical cancer tissues than in paracancerous tissues, which is negatively associated with the survival rate of patients with cervical cancer (34). The upregulation of HCP5 has been observed in prostate cancer, eventually resulting in tumor metastasis (35). Increased HCP5 levels have also been found in oral squamous cell carcinoma, and it has been shown to be significantly associated with lymph node metastasis and an advanced TNM stage (36). In the present study, it was

discovered that HCP5 was upregulated in RB tissues and cells compared to the controls. Concurrently, it was found that a high expression of HCP5 was closely associated with TNM stage and lymph node metastasis. In addition, strong associations were identified between enhanced HCP5 and IIRC stage/RE stage, suggesting that HCP5 may be an onco-lncRNA in RB.

HCP5 plays a vital role in the cellular processes of several human cancers (19,20,37). Wang *et al* revealed that the downregulation of HCP5 suppressed the proliferation of triple-negative breast cancer (TNBC) cells *in vitro* and the tumor growth of TNBC *in vivo* (37). Bai *et al* indicated that HCP5 silencing suppressed the progression of CRC *in vivo* (19). Wang *et al* demonstrated that the knockdown of HCP5 greatly contributed to the inhibition of the proliferation, migration and invasion of OC cells (20). In the present study, the proliferation, migration and invasion of RB cells, as well as the growth of tumor xenografts were suppressed by HCP5 downregulation. Based on these results, it can be conjectured that the silencing of HCP5 acts as a suppressor in the progression of Rb.

miR-3619-5p plays an anti-tumor role in the malignancy of several cancers (38,39). For instance, miR-3619-5p is minimally expressed in non-small cell lung cancer (NSCLC) tissues, whereas the overexpression of miR-3619-5p suppresses the growth and invasion of NSCLC cells *in vitro* (38). A high expression of miR-3619-5p suppresses the proliferation, migration and invasion of breast cancer cells (39). In the present study, a decreased miR-3619-5p expression was identified in RB tissues, and the upregulation of miR-3619-5p exerted suppressive effects on the proliferation and metastasis of RB cells. A recent study by Yan *et al* revealed that the proliferation, migration and invasion of RB cells were impeded by transfection with miR-3619-5p mimics (25). These results suggest that miR-3619-5p may also be function as an anti-tumor miRNA in RB. In addition, miR-3619-5p interacts with lncRNAs and is involved in cancer progression, such as LINC00202-miR-3619-5p in RB (25), DGCR5-miR-3619-5p in gallbladder cancer (40) and PVT1-miR-3619-5p in gastric cancer (41). We hypothesised that the anti-tumour function of miR-3619-5p in RB may also be regulated by HCP5. Herein, miR-3619-5p was initially identified as a target of and was negatively modulated by HCP5. The results of the present study demonstrated that the reduction of the proliferation and metastasis of Y79 cells transfected with sh-HCP5 was reversed by transfection with miR-3619-5p inhibitor. These results suggest that the silencing of HCP5 attenuates RB carcinogenicity by interacting with miR-3619-5p.

In recent years, increasing attention has been paid to the involvement of HDAC9 in the pathological process of RB (27,29). Xu *et al* suggested that HDAC9 expression was increased in RB tissues, and its downregulation inhibited the proliferation, migration and invasion of RB cells (29). In addition, Zhang *et al* confirmed that the silencing of HDAC9 suppressed the proliferation of RB cells *in vitro* (27). Consistent with these studies, an increased expression of HDAC9 was identified in the present study, indicating the oncogenicity of HDAC9 in RB. Simultaneously, it was found that HDAC9 was a target gene of and was negatively regulated by miR-3619-5p, and a positive correlation was observed between HDAC9 and HCP5 expression in RB tissues. Therefore, it was demonstrated miR-3619-5p is involved in the tumorigenesis of Rb through regulation by HCP5. It was further hypothesized that HDAC9 may also be modulated by HCP5 to play a role in the progression of Rb. Feedback verification experiments revealed that the inhibitory effects of HCP5 knockdown on the proliferation, migration and invasion of Y79 cells were reversed by HDAC9 overexpression, which confirmed this hypothesis. It was concluded that the downregulation of HCP5 suppressed the progression of Rb by sponging miR-3619-5p and regulating HDAC9. However, there may be a limitation in to the presents tudy. Only one Rb cell line (Y79) was used to perform the feedback verification experiments, and further experiments using other cell lines are required to validate this conclusion.

In conclusion, the present study demonstrates that HCP5 acts as an endogenous sponge of miR-3619-5p to regulate HDAC9. The knockdown of HCP5 mitigates the progression of RB by regulating the miR-3619-5p/HDAC9 axis. Overall, the present study provides perspectives for novel therapeutic targets for RB.

Acknowledgements

Not applicable.

Funding

The present study was funded by the Shandong Medical and Health Science and Technology Development Project (Project name: Study on the mechanism of mirNA-21 on retinal microvascular endothelial cells of RF/6A in diabetic rats; no. 2019WS599).

Availability of data and materials

The datasets used and/or analyzed during the current study are available from the corresponding author on reasonable request.

Authors' contributions

YZ made substantial contributions to the conception and design of the study, data acquisition, the drafting of the article, and gave final approval of the version to be published. FH made substantial contributions to the conception and design of the study, data analysis and interpretation, and in the drafting of the article. Both authors read and approved the final manuscript.

Ethics approval and consent to participate

The present study was approved by the Ethics Committee of Affiliated Hospital of Weifang Medical University [No. 2020(12)]. Written informed consent was obtained from all the patients. The study was conducted in accordance with the Declaration of Helsinki. The animal experiments were approved by the Ethics Committee of Affiliated Hospital of Weifang Medical University, and were performed in accordance with the institutional guide for the care and use of laboratory animals (National Institutes of Health).

Patient consent for publication

Not applicable.

Competing interests

The authors declare that they have no competing interests.

References

1. Villegas VM, Hess DJ, Wildner A, Gold AS and Murray TG: Retinoblastoma. Curr Opin Ophthalmol 24: 581-588, 2013.
2. Cimino PJ, Robirds DH, Tripp SR, Pfeifer JD, Abel HJ and Duncavage EJ: Retinoblastoma gene mutations detected by whole exome sequencing of merkel cell carcinoma. Mod Pathol 27: 1073-1087, 2014.
3. Venkatesan N, Deepa PR, Khetan V and Krishnakumar S: Computational and in vitro investigation of miRNA-Gene regulations in retinoblastoma pathogenesis: miRNA mimics strategy. Bioinform Biol Insights 9: 89-101, 2015.
4. Dimaras H, Corson TW, Cobrinik D, White A, Zhao J, Munier FL, Abramson DH, Shields CL, Chantada GL, Njuguna F and Gallie BL: Retinoblastoma. Nat Rev Dis Primers 1: 15021, 2015.
5. Okimoto S and Nomura K: Clinical manifestations and treatment of retinoblastoma in Kobe children's hospital for 16 years. J Pediatr Ophthalmol Strabismus 51: 222-229, 2014.
6. Abu-Ain MS, Shatnawi R, Yousef YA and Watts P: Heterochromia irides and mistaken identity of retinoblastoma. BMJ Case Rep 12: e231091, 2019.
7. Jenkinson H: Retinoblastoma: Diagnosis and management-the UK perspective. Arch Dis Child 100: 1070-1075, 2015.
8. Rao R and Honavar SG: Retinoblastoma. Indian J Pediatr 84: 937-944, 2017.
9. Sullivan EM, Wilson MW, Billups CA, Wu J, Merchant TE, Brennan RC, Haik BG, Shulkin B, Free TM, Given V, *et al*: Pathologic risk-based adjuvant chemotherapy for unilateral retinoblastoma following enucleation. J Pediatr Hematol Oncol 36: e335-e340, 2014.
10. Qaddoumi I, Nawaiseh I, Mehyar M, Razzouk B, Haik BG, Kharma S, Jaradat I, Rodriguez-Galindo C and Wilson MW: Team management, twinning, and telemedicine in retinoblastoma: A 3-tier approach implemented in the first eye salvage program in Jordan. Pediatr Blood Cancer 51: 241-244, 2008.
11. Chantada GL, Dunkel IJ, Schaiquevich PS, Grynszpancholc EL, Francis J, Ceciliano A, Zubizarreta PA, Fandiño AC and Abramson DH: Twenty-Year collaboration between north American and South American retinoblastoma programs. J Glob Oncol 2: 347-352, 2016.
12. Wang X, Arai S, Song X, Reichart D, Du K, Pascual G, Tempst P, Rosenfeld MG, Glass CK and Kurokawa R: Induced ncRNAs allosterically modify RNA-binding proteins in cis to inhibit transcription. Nature 454: 126-130, 2008.
13. Fatica A and Bozzoni I: Long non-coding RNAs: New players in cell differentiation and development. Nat Rev Genet 15: 7-21, 2014.
14. He X, Chai P, Li F, Zhang L, Zhou C, Yuan X, Li Y, Yang J, Luo Y, Ge S, *et al*: A novel LncRNA transcript, RBAT1, accelerates tumorigenesis through interacting with HNRNPL and cis-activating E2F3. Mol Cancer 19: 115, 2020.
15. Han S, Song L, Chen Y, Hou M, Wei X and Fan D: The long non-coding RNA ILF3-AS1 increases the proliferation and invasion of retinoblastoma through the miR-132-3p/SMAD2 axis. Exp Cell Res 393: 112087, 2020.
16. Dong Y, Wan G, Yan P, Qian C, Li F and Peng G: Long noncoding RNA LINC00324 promotes retinoblastoma progression by acting as a competing endogenous RNA for microRNA-769-5p, thereby increasing STAT3 expression. Aging (Albany NY) 12: 7729-7746, 2020.
17. Vernet C, Ribouchon MT, Chimini G, Jouanolle AM, Sidibe I and Pontarotti P: A novel coding sequence belonging to a new multicopy gene family mapping within the human MHC class I region. Immunogenetics 38: 47-53, 1993.
18. Liu Y, Helms C, Liao W, Zaba LC, Duan S, Gardner J, Wise C, Miner A, Malloy MJ, Pullinger CR, *et al*: A genome-wide association study of psoriasis and psoriatic arthritis identifies new disease loci. PLoS Genet 4: e1000041, 2008.
19. Bai N, Ma Y, Zhao J and Li B: Knockdown of lncRNA HCP5 suppresses the progression of colorectal cancer by miR-299-3p/PFN1/AKT axis. Cancer Manag Res 12: 4747-4758, 2020.
20. Wang L, He M, Fu L and Jin Y: Role of lncRNAHCP5/microRNA-525-5p/PRC1 crosstalk in the malignant behaviors of ovarian cancer cells. Exp Cell Res 394: 112129, 2020.
21. Yuan B, Guan Q, Yan T, Zhang X, Xu W and Li J: LncRNA HCP5 regulates pancreatic cancer progression by miR-140-5p/CDK8 axis. Cancer Biother Radiopharm 35: 711-719, 2020.
22. Wan W, Long Y, Li Q, Jin X, Wan G, Zhang F, Lv Y, Zheng G, Li Z and Zhu Y: MiR-25-3p promotes malignant phenotypes of retinoblastoma by regulating PTEN/Akt pathway. Biomed Pharmacother 118: 109111, 2019.
23. Li J and You X: MicroRNA758 inhibits malignant progression of retinoblastoma by directly targeting PAX6. Oncol Rep 40: 1777-1786, 2018.
24. Hao P, Yue F, Xian X, Ren Q, Cui H and Wang Y: Inhibiting effect of MicroRNA-3619-5p/PSMD10 axis on liver cancer cell growth in vivo and in vitro. Life Sci 254: 117632, 2020.
25. Yan G, Su Y, Ma Z, Yu L and Chen N: Long noncoding RNA LINC00202 promotes tumor progression by sponging miR-3619-5p in retinoblastoma. Cell Struct Funct 44: 51-60, 2019.
26. Parra M and Verdin E: Regulatory signal transduction pathways for class IIa histone deacetylases. Curr Opin Pharmacol 10: 454-460, 2010.
27. Zhang Y, Wu D, Xia F, Xian H, Zhu X, Cui H and Huang Z: Downregulation of HDAC9 inhibits cell proliferation and tumor formation by inducing cell cycle arrest in retinoblastoma. Biochem Biophys Res Commun 473: 600-606, 2016.
28. Jin Q, He W, Chen L, Yang Y, Shi K and You Z: MicroRNA-101-3p inhibits proliferation in retinoblastoma cells by targeting EZH2 and HDAC9. Exp Ther Med 16: 1663-1670, 2018.
29. Xu L, Li W, Shi Q, Wang M, Li H, Yang X and Zhang J: MicroRNA936 inhibits the malignant phenotype of retinoblastoma by directly targeting HDAC9 and deactivating the PI3K/AKT pathway. Oncol Rep 43: 635-645, 2020.
30. TNM8: The updated TNM classification for retinoblastoma. Community Eye Health 31: 34, 2018.
31. Shields CL and Shields JA: Basic understanding of current classification and management of retinoblastoma. Curr Opin Ophthalmol 17: 228-234, 2006.
32. Yousef YA, Al-Hussaini M, Mehyar M, Sultan I, Jaradat I, AlRawashdeh K, Khurma S, Deebajah R and Nawaiseh I: Predictive value of tnm classification, international classification, and reese-ellsworth staging of retinoblastoma for the likelihood of high-risk pathologic features. Retina 35: 1883-1889, 2015.
33. Livak KJ and Schmittgen TD: Analysis of relative gene expression data using real-time quantitative PCR and the 2(-Delta Delta C(T)) method. Methods 25: 402-408, 2001.
34. Yu Y, Shen HM, Fang DM, Meng QJ and Xin YH: LncRNA HCP5 promotes the development of cervical cancer by regulating MACC1 via suppression of microRNA-15a. Eur Rev Med Pharmacol Sci 22: 4812-4819, 2018.
35. Hu R and Lu Z: Long noncoding RNA HCP5 promotes prostate cancer cell proliferation by acting as the sponge of miR4656 to modulate CEMIP expression. Oncol Rep 43: 328-336, 2020.
36. Zhao J, Bai X, Feng C, Shang X and Xi Y: Long non-coding RNA HCP5 facilitates cell invasion and epithelial-mesenchymal transition in oral squamous cell carcinoma by miR-140-5p/SOX4 axis. Cancer Manag Res 11: 10455-10462, 2019.
37. Wang L, Luan T, Zhou S, Lin J, Yang Y, Liu W, Tong X and Jiang W: LncRNA HCP5 promotes triple negative breast cancer progression as a ceRNA to regulate BIRC3 by sponging miR-219a-5p. Cancer Med 8: 4389-4403, 2019.
38. Niu X, Liu S, Jia L and Chen J: Role of MiR-3619-5p in β-catenin-mediated non-small cell lung cancer growth and invasion. Cell Physiol Biochem 37: 1527-1536, 2015.
39. Lv MH, Mao QX, Li JT, Qiao J, Chen X and Luo S: Knockdown of LINC00665 inhibits proliferation and invasion of breast cancer via competitive binding of miR-3619-5p and inhibition of catenin beta 1. Cell Mol Biol Lett 25: 43, 2020.
40. Liu S, Chu B, Cai C, Wu X, Yao W, Wu Z, Yang Z, Li F, Liu Y, Dong P and Gong W: DGCR5 promotes gallbladder cancer by sponging MiR-3619-5p via MEK/ERK1/2 and JNK/p38 MAPK pathways. J Cancer 11: 5466-5477, 2020.
41. Wu C, Hu Y, Ning Y, Zhao A, Zhang G and Yan L: Long noncoding RNA plasmacytoma variant translocation 1 regulates cisplatin resistance via miR-3619-5p/TBL1XR1 axis in gastric cancer. Cancer Biother Radiopharm 35: 741-752, 2020.